JOURNAL OF Materials CHEMISTRY

Crystallization mechanism of Al–Ti-beta zeolite synthesized from amorphous wetness impregnated xerogels

David P. Serrano,* Maria A. Uguina, Gabriel Ovejero, Rafael van Grieken, Marta Camacho and Juan A. Melero

Department of Chemical Engineering, Faculty of Chemistry, Complutense University of Madrid, 28040 Madrid, Spain. E-mail: rada@eucmax.sim.ucm.es

Received 21st May 1999, Accepted 3rd August 1999

The crystallization mechanism of Al–Ti-beta zeolite has been investigated when this material is synthesized from amorphous SiO_2–TiO_2 xerogels wetness impregnated with NEt_4OH solutions. The final crystalline product presents most of the titanium atoms occupying tetrahedral positions in the framework as concluded from DR UV-VIS spectra, whereas bulk TiO_2 phases are not detected. Likewise,^{27}Al MAS-NMR indicates the presence of Al with tetrahedral coordination in the Al–Ti-beta framework. The use of Al isopropoxide as the aluminium source leads to shorter synthesis times and higher incorporation degrees of aluminium compared to Al nitrate. The crystallization mechanism involves dissolution of the raw xerogel and subsequent formation of an amorphous gel consisting of primary particles with sizes around 10 nm. The appearance of the first crystallization nuclei is closely related to the incorporation of Al into these primary units. Both crystallinity and solid yield increase initially very rapidly until total incorporation of the Al species into the solid phase occurs. Thereafter, the primary particles undergo an aggregation process into larger secondary units. The last crystallization stage is characterized by slow incorporation of silicon and titanium species from the solution with a slight increase in the solid yield, which results in a densification of the secondary particles and their transformation into zeolite crystals.

1 Introduction

The incorporation of Ti atoms in framework positions of zeolites has received much attention in the past decade as the obtained materials have proved to be efficient selective oxidation catalysts. TS-1 (MFI structure, medium pore zeolite) shows a high activity and selectivity in oxidation reactions of different substrates (olefins, alkanes, alcohols, ketones, aromatics, *etc.*) with hydrogen peroxide.[1] However, the use of TS-1 is restricted to the oxidation of relatively small organic molecules using hydrogen peroxide as oxidant due to diffusion limitations and size exclusion effects. An important step forward in this field was the synthesis of the first large-pore zeolite containing titanium, namely Al–Ti-beta.[2] This new material made feasible the oxidation of bulkier substrates with hydrogen peroxide[2,3] and also the possibility of using organic hydroperoxides as an oxygen source.[4]

Crystallization of Al–Ti-beta zeolite in a basic medium using tetraethylammonium hydroxide as the structure-directing agent requires the presence of Al or the incorporation of zeolite seeds. In addition to the conventional hydrothermal synthesis from a basic liquid gel,[2] a variety of alternatives have been developed for the preparation of Al–Ti-beta: wetness impregnation of xerogels,[5,6] seeding techniques[7] and gas–solid[8] and liquid–solid[9] isomorphous substitution.

Although the presence of aluminium in Al–Ti-beta may be useful for bifunctional acid/redox catalytic processes,[10] the acid sites seem to lower its activity and selectivity in oxidation reactions.[3] In this way, synthetic efforts have been directed towards widening the range of Si : Al molar ratios of this zeolite beyond the limits established in the original patent[11] (Si : Al = 5–100 : 1), based on dealuminization processes or seeding techniques.[7] Recently, Camblor *et al.*[12] have reported the first unseeded synthesis method for the preparation of all silica zeolite beta in a fluoride medium. This new method has also been used successfully in the synthesis of Al-free Ti-beta.[13,14] This material has a high hydrophobic character in comparison to those synthesized by wetness impregnation and conventional methods, which is an important feature from a catalytic point of view.

In contrast with the high number of works dealing with the catalytic properties of Ti containing zeolites, little research effort has been devoted to the study of their crystallization mechanism. In previous works on the synthesis of TS-1 and TS-2 zeolites from amorphous wetness impregnated SiO_2–TiO_2 xerogels,[15,16] we have found that in this case the crystallization proceeds mainly through solid–solid transformations. This finding was in contrast with the conventional mechanism which postulates that the zeolite synthesis proceeds through two main steps: nucleation (formation of the first and very small crystalline entities) and crystal growth around these nuclei by progressive incorporation of soluble species. As will be shown in this work, the crystallization mechanism of Al–Ti-beta from amorphous xerogels is different from that of TS-1 and TS-2 zeolites, although the classical step of crystal growth by simple incorporation of soluble species is not observed. On the contrary, the zeolite crystals are initially formed by aggregation of amorphous primary particles with sizes around 10 nm and subsequent densification and zeolitization of the resulting secondary units.

2 Experimental

2.1 Sample preparation

The amorphous SiO_2–TiO_2–Al_2O_3 mixed oxides used as raw materials for the Al–Ti-beta synthesis were prepared following a two step sol–gel process similar to those earlier applied for the preparation of TS-1 and Al-TS-1 zeolites.[17,18] Tetraethyl orthosilicate (TEOS, Alfa) was first prehydrolysed at room temperature in an acidic medium before addition of the aluminium source (aluminium isopropoxide, AIP, Aldrich; $Al(NO_3)_3 \cdot 9H_2O$, Panreac). Then, the mixture was cooled at 0 °C and a solution of titanium tetrabutoxide (TNBT, Alfa) in

Table 1 Influence of the Al source and addition procedure

	Starting xerogel			Impregnating solution		
Sample	Based on	Al Source	Si : Al Molar ratio	Based on	Si : Al Molar ratio	X_c (%)[a]
1	SiO_2–TiO_2–Al_2O_3	AIP	193	20 wt% NEt_4OH	No Al	No solid
2	SiO_2–TiO_2–Al_2O_3	Al nitrate	193	20 wt% NEt_4OH	No Al	0
3	SiO_2–TiO_2–Al_2O_3	AIP	193	20 wt% NEt_4OH + Al nitrate	50	100
4	SiO_2–TiO_2–Al_2O_3	AIP	193	20 wt% NEt_4OH + AIP	100	100
5	SiO_2–TiO_2	—	No Al	20 wt% NEt_4OH + AIP	50	100
6	SiO_2–TiO_2	—	No Al	20 wt% NEt_4OH + Al nitrate	50	65

Si : Ti molar ratio in the initial xerogel = 30 : 1. Synthesis conditions: 135 °C; 7 d; W = 3 g per g. [a]Crystallinity.

isopropyl alcohol added dropwise. In a second step the gelation was accelerated by addition of 20 wt% aqueous NEt_4OH, the cogel obtained being dried at 110 °C overnight and crushed to give a powdered material. Obviously, in the preparation of amorphous SiO_2–TiO_2 xerogels, the aluminium addition was omitted.

Al–Ti-beta synthesis was carried out by thermal treatment under autogenous pressure of the corresponding cogel after being wetness impregnated with a 20 wt% aqueous NEt_4OH solution (solution : xerogel mass ratio, W = 3.0). Al–Ti-beta requires the presence of Al ions to crystallize when NEt_4OH is used as directing agent. These aluminium species can be added together with the template impregnating solution and/or in the raw material. After impregnation, the incipient wet cogel was charged into Teflon-lined autoclaves and crystallized under autogenous pressure at 135 °C over different time periods (10 h–7 d). After this treatment, the solid product of the synthesis was recovered according to the size of the particles. Solids with very low particle size were separated by the use of microfiltration membranes whereas materials with larger particles were separated by centrifugation. After separation, the solid was washed several times with distilled water and dried overnight at 110 °C. The calcination of the samples was carried out in air at 550 °C for 7 h.

2.2 Characterization

Chemical analyses of the samples were performed by X-ray fluorescence (XRF) with a Philips PW 1480 spectrometer. X-Ray diffraction (XRD) patterns were collected with a Philips X'PERT diffractometer with Cu-Kα radiation. Fourier transform IR (FT-IR) spectra were recorded by means of a Nicolet 510P spectrophotometer using the KBr wafer technique. The crystallinity of the samples was determined from both the XRD peak area between 2θ = 20 and 24° and the ratio between the intensities in absorbance units of the 550 and 800 cm^{-1} IR bands, using a highly crystalline Al–Ti-beta sample as reference.

Diffuse reflectance UV-VIS spectra (DR UV-VIS) were obtained under ambient conditions on a CARY-1 spectrophotometer equipped with a diffuse reflectance accessory. ^{27}Al magic angle spinning nuclear magnetic resonance (MAS-NMR) spectra of powdered samples were recorded at 78.14 MHz in a Varian VXR-300, with a spinning frequency of 4000 Hz and time intervals of 5 s between successive accumulations. Measurements were made at room temperature with $[Al(H_2O)_6]^{3+}$ as external standard reference with 400 accumulations.

The BET (Brunauer–Emmett–Teller) surface area, micropore volume and pore size distribution of the different materials were obtained from nitrogen adsorption–desorption measurements at 77 K using the volumetric method (Micromeritics, ASAP 2000). The morphology and size of the crystallites were determined by transmission electronic microscopy (TEM) with a JEOL JEM-200 FX microscope and scanning electronic microscopy (SEM) with a JEOL JSM-6400 microscope.

3 Results and discussion

3.1 Preliminary experiments

Preliminary experiments were carried out in order to establish the optimum conditions for the Al–Ti-beta synthesis from wetness-impregnated silica based xerogels. In this way the influence of different aluminium sources and the Al addition mode to the synthesis medium were studied.

Table 1 summarizes the synthesis conditions and crystallinity (X_c) of different Al–Ti-beta samples prepared from wetness impregnated amorphous xerogels. When starting from SiO_2–TiO_2–Al_2O_3 xerogels with a Si : Al molar ratio of 193 : 1 (Table 1; samples 1 and 2), no crystalline products were obtained after seven days of synthesis, either using AIP as aluminium source or with $Al(NO_3)_3{\cdot}9H_2O$. However, when the amount of Al was increased through its incorporation in the impregnating solution (Table 1; samples 3 and 4), the materials obtained showed high crystallinities, *ca.* 100%. These results confirm that the Al species play an important role in Al–Ti-beta synthesis from xerogels, an effect which has been also observed in conventional methods, leading to the conclusion that the Al species are essential for the nucleation of the BEA phase.[19]

When the synthesis is carried out by wetness impregnation of a SiO_2–TiO_2 amorphous xerogel with a solution of NEt_4OH including the aluminium source (Table 1; sample 5) highly crystalline material is also obtained after 7 d of synthesis in the case of AIP. This feature suggests that the presence

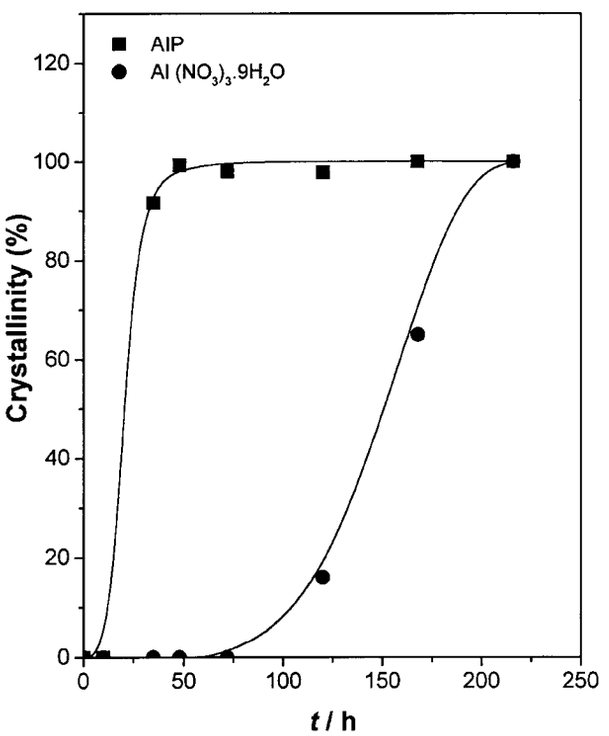

Fig. 1 Influence of the aluminium source. Crystallization kinetics.

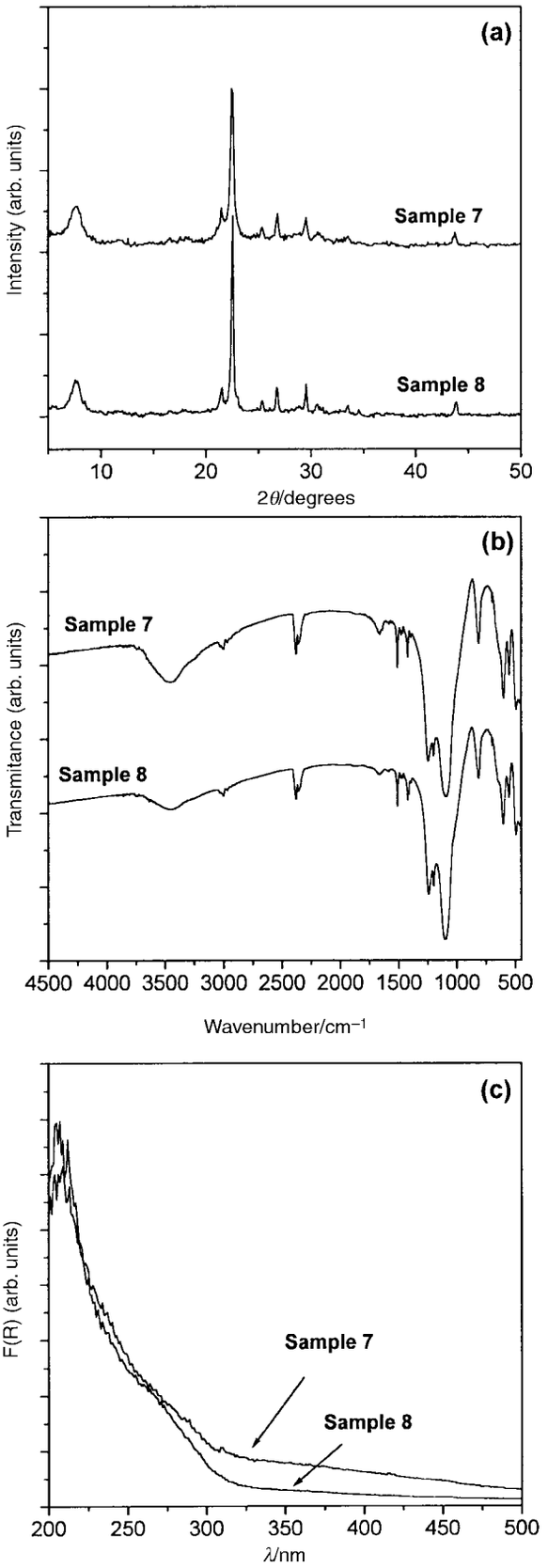

Fig. 2 Influence of the aluminium source. Characterization of the as-synthesized Al–Ti-beta samples. (a) XRD spectra, (b) FTIR spectra, (c) DR UV-VIS spectra.

of Al in the starting xerogel causes the same effect as when it is added in the impregnating solution. However, if the SiO_2–TiO_2 xerogel is wetness impregnated with a NEt_4OH solution containing $Al(NO_3)_3$·;$9H_2O$ as aluminium source (Table 1; sample 6), the zeolite obtained shows lower crystallinity after the same synthesis time, which shows the significant role of the aluminium source.

In order to study in more detail the influence of the aluminium source (AIP *versus* $Al(NO_3)_3.9H_2O$) in the synthesis of Al–Ti-beta zeolite, two series of kinetics runs were carried out (Fig. 1). In both cases, the same amorphous SiO_2–TiO_2 xerogel (Si : Ti molar ratio = 30 : 1) was used as raw material, being impregnated under identical conditions. Table 2 shows the synthesis yield, chemical molar composition and properties of the final highly crystalline materials synthesized using both aluminium sources (samples 7 and 8), whereas Fig. 1 compares the evolution of the crystallinity in both series of experiments. While the use of AIP allows one to obtain highly crystalline materials in just 24 h, when using $Al(NO_3)_3·9H_2O$ the synthesis time is increased to 216 h. This fact suggests that the AIP hydrolysis leads to aluminium species more reactive than those from $Al(NO_3)_3·9H_2O$ which allows a faster condensation and linkage to the SiO_2 network. Moreover, from the results shown in Table 2, the use of AIP favours higher aluminium incorporation during the crystallization, which also enhances the synthesis yield. However, the Ti incorporation in the final crystalline product is higher when $Al(NO_3)_3·9H_2O$ is used as aluminium source which is probably associated with the lower aluminium incorporation, and therefore a higher probability for the isomorphous substitution of silicon by titanium. This feature confirms the competitive incorporation of Ti and Al species during the synthesis, which has also been observed in the preparation of other Ti and Al containing materials, such as Al-TS-1, through conventional[20] and sol–gel methods.[21,22]

Fig. 2 illustrates the XRD, FTIR and DR UV-VIS spectra of highly crystalline samples obtained using both aluminium sources (samples 7 and 8). In both cases, materials with BEA structure were obtained as concluded from the XRD (Fig. 2a) and IR (Fig. 2b) spectra. DR UV-VIS spectroscopy is a useful technique to determine the dispersion of Ti in silica-based molecular sieves, since the presence of TiO_2 can be detected by the observance of an absorption band at 330 nm.[20,23] In addition, a narrow band centred on 220 nm is usually considered as evidence of the Ti atoms occupying tetrahedral positions in the zeolite framework.[23] In the DR UV-VIS spectra of the samples, shown in Fig. 2c, a wide band centered around 210 nm with a shoulder at 270 nm is observed, whereas no band around 330 nm is detected. These results indicate that most of the Ti atoms are present in tetrahedral positions of the zeolite framework. The signal around 270 nm has been also observed by other authors,[24] being assigned to the existence of five-coordinate titanium atoms linked to four Si–O groups and an OH^- group, the negative charge being compensated for by NEt_4^+ cations.

Fig. 3 shows SEM and TEM micrographs of both Al–Ti-

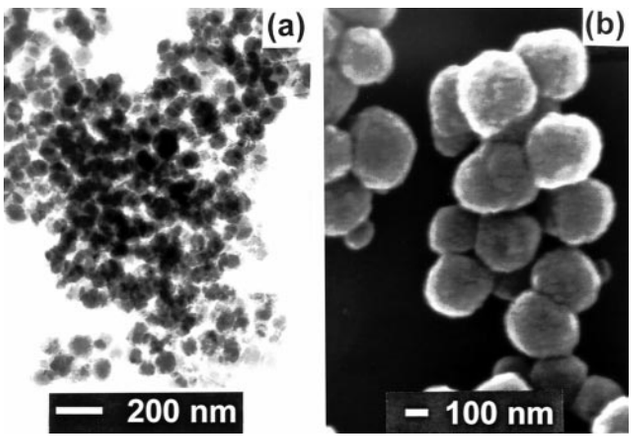

Fig. 3 Influence of the aluminium source. (a) TEM image of sample 7, (b) SEM image of sample 8.

Table 2 Influence of the Al source. Physicochemical properties of Al–Ti-beta samples

Sample	Al source	t_s[a]/h	X_c[b] (%)	η[c] (%)	Solid molar composition		Crystal size/nm
					Si/Ti	Si/Al	
7	AIP	168	100	69.5	50.0	29.5	100
8	$Al(NO_3)_3{\cdot}9H_2O$	216	98.7	61.3	37.7	39.6	300

Initial molar composition of the impregnated xerogel: Si : Ti = 30 : 1 and Si : Al = 50 : 1. Synthesis conditions: 135 °C; W = 3 g per g. [a]Synthesis time. [b]Crystallinity. [c]Synthesis yield defined as: g of calcined zeolite obtained per g of SiO_2 in the initial xerogel.

beta samples. The material synthesized using $Al(NO_3)_3{\cdot}9H_2O$ (sample 8) presents an average crystal size around 0.3 μm, which is three times higher than that of the sample synthesized using AIP as aluminium source (sample 7). This fact is in close agreement with the slower crystallization kinetics observed when Al nitrate is used as the aluminium source. The lower reactivity of the Al species coming from the $Al(NO_3)_3{\cdot}9H_2O$ hydrolysis leads to a slower nucleation and hence to the formation of larger crystals.

3.2 Crystallization mechanism of Al–Ti-beta zeolite

In order to study the mechanism of Al–Ti-beta crystallization using wetness impregnated xerogels as raw materials, a kinetic run was carried out varying the synthesis time at 135 °C and with AIP as aluminium source. The initial amorphous xerogel was a SiO_2–TiO_2–Al_2O_3 solid with Si : Ti and Si : Al molar ratios of 30 and 100 : 1, respectively. This solid was impregnated, until the incipient wetness point was reached, with an aqueous solution of NEt_4OH (20 wt%) including additional Al (Si : Al molar ratio = 100 : 1 on the basis of the initial amount of SiO_2 in the raw xerogel). Fig. 4 shows the variation of the crystallinity and solid yield corresponding to this experiment. It is remarkable that the starting polymeric xerogel is completely dissolved during the first hours of synthesis leading to a solution containing the different species. However, a few hours later a solid gel appears, formed initially by amorphous particles. From the results shown in Fig. 4, the crystallization proceeds clearly through two different steps. The first takes place with a high crystallization rate to reach values of about 80% crystallinity and up to 60% synthesis yield. In the second step the crystallinity changes from 80 to 100% whereas the solid yield increases smoothly to a constant value of *ca.* 70%.

The incorporation degree of the different elements during the synthesis, shown in Fig. 5, indicates that all the aluminium is completely consumed during the first hours of reaction. This total consumption of Al corresponds with the end of the above first step of the crystallization. Accordingly, the second stage of the crystallization process occurs without Al in the solution through just the incorporation of silicon and titanium species. This result suggests that the presence of aluminium is essential in the formation of the initial amorphous gel and its subsequent transformation, which is in agreement with the role of Al species for the nucleation of the BEA structure earlier reported.[19,25]

The incorporation of titanium and silicon also increases with the crystallization time, but in both cases it is less effective than that of Al. When 100% crystallinity is reached, these values are around 59 and 67% as regards the initial amounts present in the raw mixture (Fig. 5). However, in contrast with the Al species, the incorporation of both elements occurs throughout the crystallization. The maximum incorporation of silicon is determined by the pH of the reaction medium, which sets up the chemical equilibrium between the silicon species incorporated into the solid and the concentration of soluble silicates in solution. This maximum incorporation determines the final synthesis yield. On the other hand, the maximum Ti content is

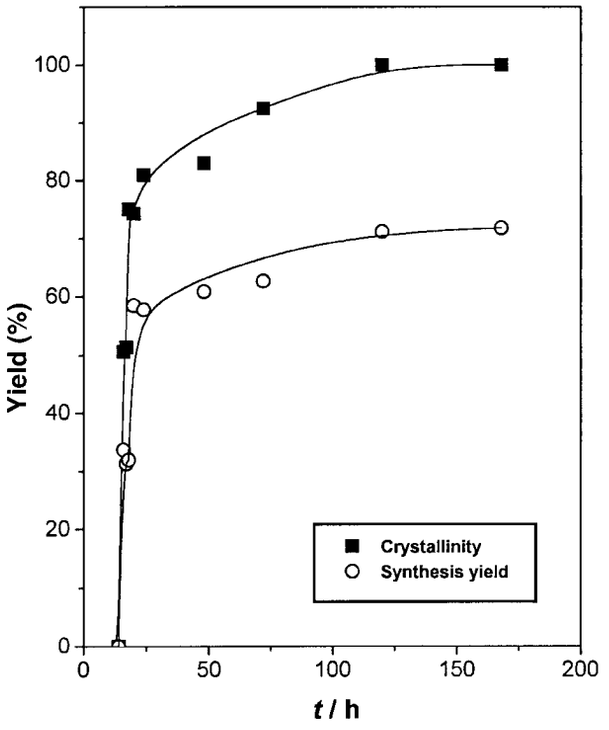

Fig. 4 Crystallization kinetics and synthesis yield of Al–Ti-beta. Molar composition of the initial xerogel: Si : Ti = 30 : 1 and Si : Al = 100 : 1, solution of NEt_4OH with additional Al (Si : Al = 100 : 1).

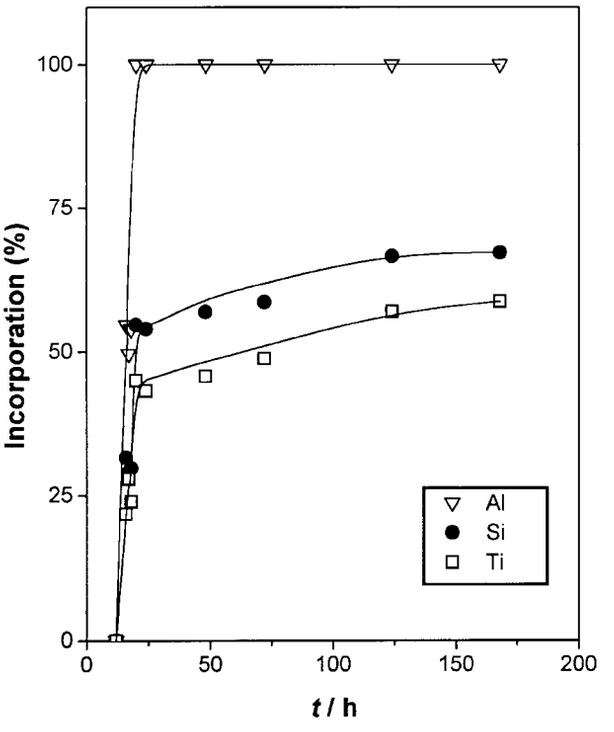

Fig. 5 Crystallization mechanism. Al, Si and Ti incorporation into the solid during the synthesis.

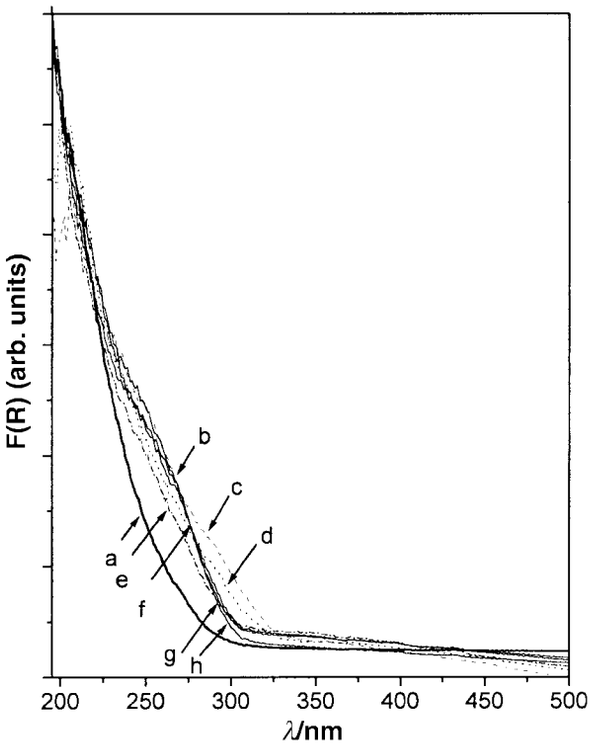

Fig. 6 Crystallization mechanism. DR UV-VIS spectra of as-synthesized samples obtained at different synthesis times: (a) starting xerogel, (b) $t=16$, (c) 17, (d) 20, (e) 24, (f) 48, (g) 72, (h) 120 h.

probably limited by the competition between Ti and Al for incorporation into the framework.

Fig. 6 shows the DR UV-VIS spectra of the as-synthesized samples obtained at different synthesis times, compared with that of the starting xerogel. The initial xerogel presents a band at 220 nm, showing that the Ti atoms are occupying tetrahedral positions in this material without evidence of TiO_2 phases. The spectra of the first partially crystalline samples (16–20 h) also do not present any absorptions related to the TiO_2 phases. However a band wider than that corresponding to the initial xerogel is observed with a shoulder around 270 nm, which evidences a higher interaction between Ti and NEt_4^+ in this solid in comparison to the initial xerogel. As the crystallization progresses the spectra become somewhat narrower, although the five-coordinated Ti species remain. Moreover, it is remarkable that the changes in the spectra are negligible as the sample crystallinity increases in the range 50–100%.

^{27}Al MAS NMR spectroscopy is a useful tool to determine the state of Al atoms in the zeolite lattice. The presence of octahedral Al atoms, usually in the form of extraframework species, is indicated by a peak centered at 0 ppm, whereas the Al atoms effectively incorporated into the zeolite framework present a peak around 50 ppm.[26] Fig. 7 shows the ^{27}Al MAS NMR spectra of the starting xerogel and several as-synthesized samples obtained at different synthesis times. In all cases the Al atoms exhibit a tetrahedral environment as concluded from the signal centred at 48 ppm and the absence of signal at 0 ppm. Interestingly, the Al environment in the partially crystalline materials is similar to that of the high crystalline samples. Likewise, as the crystallization proceeds, the signal centred around 50 ppm becomes narrower and its position is slightly shifted to higher frequencies, which is a consequence of a more homogeneous environment of the Al atoms.

Fig. 8(a) illustrates a TEM microphotograph corresponding to a partially crystalline sample, showing that it consists of small primary units with sizes around 10 nm. These primary units are aggregated into secondary particles which exhibit an irregular shape with dimensions of *ca.* 70×60 nm (Fig. 8b) for 75% crystallinity and 60% solid yield. As the crystallization progresses the secondary particles become larger by aggregation of more primary particles and become more compact by packing of these initial blocks. For a crystallinity around 80% the primary units are more difficult to distinguish and the size

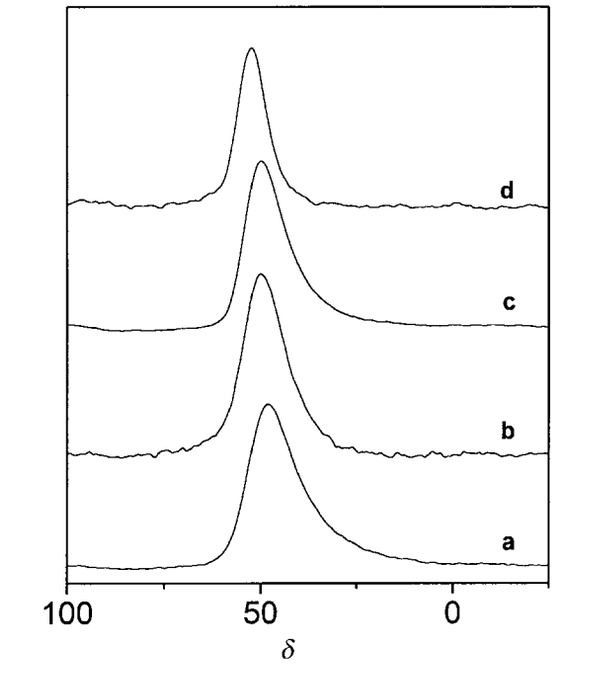

Fig. 7 Crystallization mechanism. ^{27}Al MAS-NMR spectra of as-synthesized samples obtained at different synthesis times: (a) starting xerogel, (b) $t=16$, (c) 18, (d) 168 h.

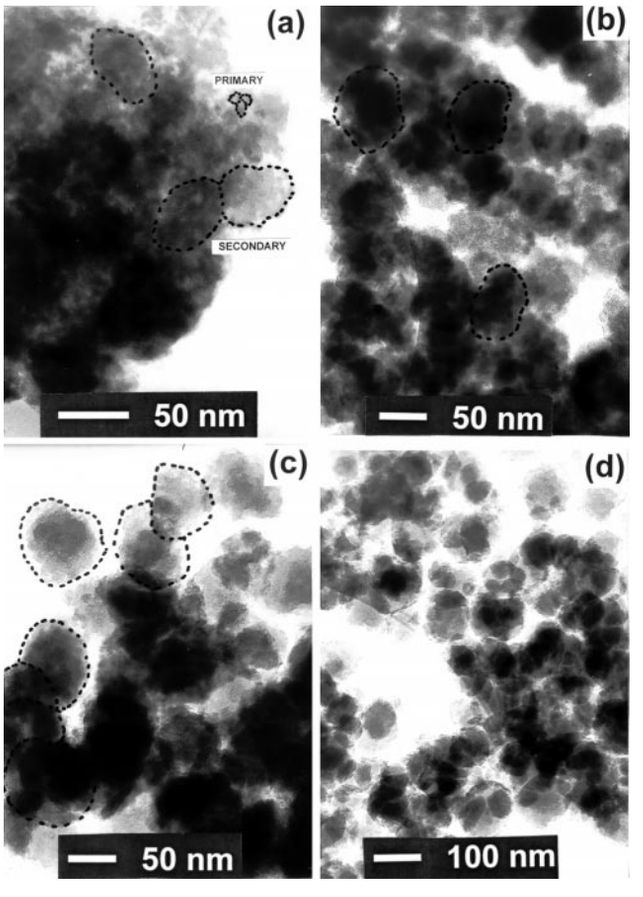

Fig. 8 Crystallization mechanism. TEM images of samples with different crystallinities: (a) $t=16$ h, $X_c=50.6\%$; (b) $t=18$ h, $X_c=75.06\%$; (c) $t=24$ h, $X_c=80.9\%$; (d) $t=120$ h, $X_c=100\%$.

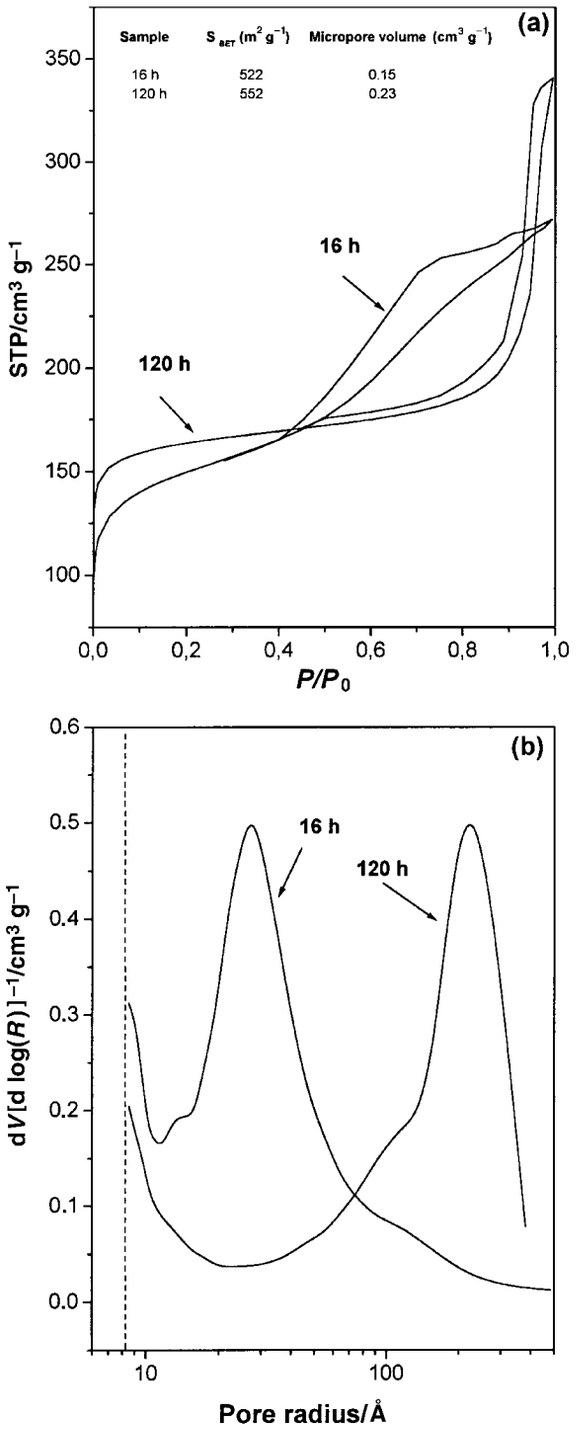

Fig. 9 Crystallization mechanism. Nitrogen adsorption isotherms at 77 K of calcined samples obtained at two different synthesis times (a) and their corresponding BJH pore size distribution in the mesoporous range (b).

of the secondary particle is around 85×75 nm (Fig. 8c). Finally, in the Al–Ti-beta samples with the highest crystallinity, crystals with sizes around 110×95 nm are present, whereas the primary units are not clearly seen. These results show that the secondary particles are transformed gradually into the final zeolite crystals through a process of densification and zeolitization (Fig. 8d).

In order to follow the changes undergone in the textural properties of these materials, N_2 adsorption isotherms at 77 K have been measured over two samples prepared at different times, 16 h ($X_c = 50$) and 120 h ($X_c = 100\%$). The results obtained are depicted in Fig. 9. The isotherm corresponding to the first sample indicates clearly the presence of mesopores attributed to the voids between the primary particles, as well as of micropores with a pore volume of 0.15 cm^3 g^{-1}, as estimated from the t-plot analysis of the isotherm. The highly crystalline sample shows a high N_2 adsorption at P/P_0 lower than 0.1, in agreement with the microporous character of this sample (0.23 cm^3 g^{-1}). The high adsorption observed at P/P_0 above 0.9 is attributed to the presence of interparticle voids. Fig. 9(b) shows the pore size distribution in the mesopore range of both samples calculated using the Barrett–Joyner–Halenda (BJH) model. The partially amorphous material ($X_c = 50\%$) shows a maximum around a pore radius of 30 Å. However, this kind of mesoporosity disappears completely in the highly crystalline material while large pores in the range 200–300 Å are observed arising from intercrystalline voids.

In the last stage of this research we increased the aluminium content in the reaction medium in order to get a deeper knowledge of this non-conventional crystallization mechanism. In this way, a second kinetic run was carried out starting from an amorphous SiO_2–TiO_2–Al_2O_3 xerogel with Si : Ti and Si : Al molar ratios of 30 and 100 : 1, respectively. This raw material was wetness impregnated with an aqueous solution of NEt_4OH (20 wt%) containing additional AIP (Si : Al molar ratio = 50 : 1 on the basis of the initial amount of SiO_2 in the raw xerogel). Table 3 shows the crystallinity, yield and chemical composition of the samples obtained in this kinetic experiment. The crystallization rate is faster as the aluminium concentration increases in the reaction medium, since highly crystalline materials are obtained in just 24 h. Regarding the synthesis yield, a remarkable fact is that this variable remains almost constant throughout the crystallization. Moreover, there is no evidence of xerogel dissolution during the first hours of reaction. All these facts indicate that the xerogel dissolution, the formation of the partially amorphous material and its subsequent evolution to crystalline materials is accelerated as the aluminium content increases in the initial mixture.

Table 3 shows the evolution of the chemical composition of the solid at different crystallization times. First, it must be pointed out that the crystalline material is just formed when a significant amount of Ti is expelled from the initial amorphous solid and all the aluminium is consumed from the solution. Thus, the highly crystalline material obtained after 24 h of synthesis presents a very low Ti incorporation with a complete incorporation of Al species. This fact shows again the competitive effect between both elements and how the Ti incorporation is lowered when the aluminium content is increased in the reaction medium.[22] As the crystallization progresses (times >24 h) an important increase of the Ti content of the solid is observed. However, this increase is produced by the precipitation of amorphous TiO_2, as concluded from the absorption band centred at 330 nm observed in the DR UV-VIS spectra of the samples obtained at long synthesis time (Fig. 10). In the presence of a high concentration of aluminium, the number of vacancies for the

Table 3 Influence of the aluminium content on the crystallization mechanism

			Solid molar composition	
t_s/h	X_c[a] (%)	η[b] (%)	Si/Ti	Si/Al
12	0	66.8	42.0	21.6
18	0	62.3	61.9	20.8
24	100	61.1	95.8	20.9
48	100	62.6	69.0	21.4
96	100	68.2	34.7	21.5

Molar composition of the initial impregnated xerogel: Si : Ti = 30 : 1, Si : Al = 28.4 : 1. Synthesis conditions: 135 °C; $W = 3$ g per g. [a]Crystallinity. [b]Synthesis yield defined as: g of calcined zeolite obtained per g of SiO_2 in the initial xerogel.

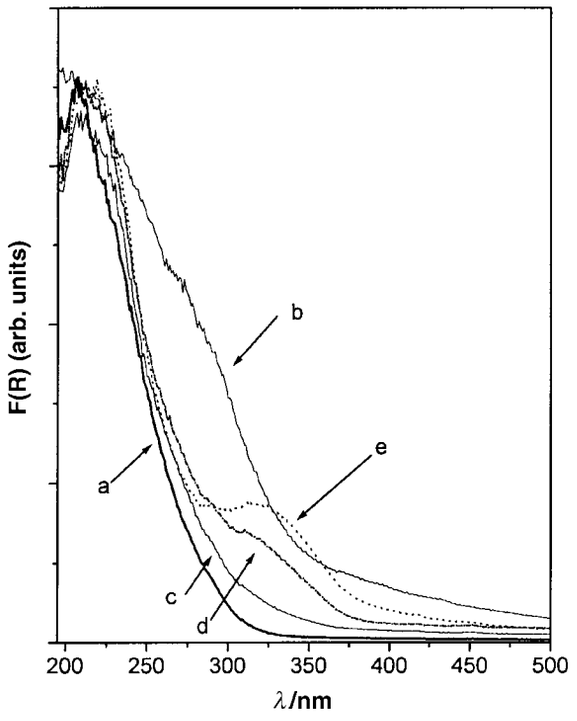

Fig. 10 DR UV-VIS spectra of as-synthesized samples obtained at different synthesis times (molar composition of the initial xerogel: Si : Ti = 30 : 1 and Si : Al = 100 : 1; solution of NEt_4OH with additional Al (Si : Al = 50 : 1): (a) starting xerogel, (b) $t = 18$, (c) 24, (d) 48, (e) 96 h.

isomorphous substitution of Ti atoms into the framework is very low, the excess being precipitated as extraframework TiO_2.

4 Conclusion: proposed mechanism of crystallization

According to the results obtained, the Al–Ti-beta crystallization from amorphous wetness impregnated silica based xerogels can be described by the following steps. Step 1: the starting polymeric xerogel is completely dissolved during the first hours of synthesis. Step 2: an amorphous solid gel consisting of primary particles with sizes around 10 nm is formed. This phase is rich in aluminium species, which limits the Ti incorporation. The coordination of Al and Ti atoms in this amorphous phase is mainly tetrahedral. Nucleation of zeolite beta takes place on this phase closely related to the Al species. Step 3: crystal growth by aggregation. Secondary particles are formed by aggregation of the primary ones and the first signs of crystallinity are detected. At the end of this stage, characterized by the total consumption of Al from the solution, the secondary particles reach sizes around 85×75 nm with crystallinities of *ca.* 80%. Step 4: growth and densification of the secondary particles through the incorporation of soluble silicon and titanium species. This stage is the slowest one leading to crystallinity of *ca.* 100% through a true liquid phase transport.

In agreement with this scheme, Al–Ti-beta crystallization from wetness impregnated amorphous silica based xerogels proceeds by a non-conventional mechanism. In contrast with the classical two-step process (nucleation–crystal growth from soluble species) usually proposed to describe the zeolite synthesis, in the system here studied the crystals are formed by aggregation, densification and zeolitization of amorphous primary particles. The increase in the Al content accelerates step 2 of the mechanism, as it favours the zeolite beta nucleation. A fast crystallization is also promoted by the use of Al isopropoxide instead of Al nitrate, which is probably due to the higher reactivity of the species coming from the alkoxide hydrolysis.

Acknowledgements

This work has been partially funded by CICYT (Comisión Interministerial de Ciencia y Tecnología), project MAT 96/0924.

References

1 G. Bellussi and M. S. Rigutto, in *Advanced Zeolite Science and Applications*, eds. J. C. Jansen, M. Stöcker, H. G. Karge and J. Weitkamp, Elsevier, Amsterdam, 1994.
2 M. A. Camblor, A. Corma, A. Martínez and J. Pérez-Pariente, *J. Chem. Soc., Chem. Commun.*, 1992, 589.
3 A. Corma, M. A. Camblor, P. Esteve, A. Martínez and J. Pérez-Pariente, *J. Catal.*, 1994, **145**, 151.
4 A. Corma, P. Esteve, A. Martínez and S. Valencia, *J. Catal.*, 1995, **152**, 18.
5 M. A. Uguina, G. Ovejero, R. Van Grieken, D. P. Serrano and M. Camacho, *Stud. Surf. Sci. Catal.*, 1995, **98**, 24.
6 M. A. Camblor, M. Constantini, A. Corma, P. Esteve, L. Gilbert, A. Martínez and S. Valencia, *Appl. Catal.*, 1995, **133**, L185.
7 M. A. Camblor, M. Constantini, A. Corma, L. Gilbert, P. Esteve, A. Martínez and S. Valencia, *Chem. Commun.*, 1996, 1339.
8 M. S. Rigutto, R. de Rueter, J. P. M. Niederer and H. van Bekkum, *Stud. Surf. Sci. Catal.*, 1994, **84**, 2245.
9 J. S. Reddy and A. Sayari, *J. Chem. Soc., Chem. Commun.*, 1995, 23.
10 A. Corma, M. Iglesias and F. Sánchez, *J. Chem. Soc., Chem. Commun.*, 1995, 1635.
11 R. L. Wadlinger, G. T. Kerr and E. J. Rosinski, U.S. Pat., 3 308 069, 1967.
12 M. A. Camblor, A. Corma and S. Valencia, *Chem. Commun.*, 1996, 2635.
13 T. Blasco, M. A. Camblor, A. Corma, P. Esteve, A. Martínez, C. Prieto and S. Valencia, *Chem. Commun.*, 1996, 2367.
14 T. Blasco, M. A. Camblor, A. Corma, P. Esteve, J. M. Guil, A. Martínez, J. A. Perdigón-Melón and S. Valencia, *J. Phys. Chem.*, 1998, **102**, 75.
15 D. P. Serrano, M. A. Uguina, G. Ovejero, R. van Grieken and M. Camacho, *Microporous Mater.*, 1996, **7**, 309.
16 D. P. Serrano, M. A. Uguina, G. Ovejero, R. Van Grieken and M. Camacho, *Chem. Commun.*, 1996, 1907.
17 M. A. Uguina, G. Ovejero, R. van Grieken, D. P. Serrano and M. Camacho, *J. Chem. Soc., Chem. Commun.*, 1994, 27.
18 G. Ovejero, R. van Grieken and J. A. Melero, *Microporous Mesoporous Mater.*, 1998, **22**, 638.
19 M. A. Camblor, A. Corma and J. Pérez-Pariente, *Zeolites*, 1993, **13**, 82.
20 G. Bellussi, A. Carati, M. G. Clerici and A. Esposito, *Stud. Surf. Sci. Catal.*, 1991, **63**, 241.
21 G. Ovejero, R. van Grieken, M. A. Uguina, D. P. Serrano and J. A. Melero, *Catal. Lett.*, 1996, **41**, 69.
22 G. Ovejero, R. van Grieken, M. A. Uguina, D. P. Serrano and J. A. Melero, *J. Mater. Chem.*, 1998, **8**, 2269.
23 F. Geobaldo, S. Bordiga, A. Zecchina, E. Gianello, G. Leofanti and G. Petrini, *Catal. Lett.*, 1992, **16**, 109.
24 T. Blasco, M. A. Camblor, A. Corma and J. Pérez-Pariente, *J. Am. Chem. Soc.*, 1993, **115**, 11806.
25 S. L. Jahn, P. A. P. Nascente and D. Cardoso, *Zeolites*, 1997, **19**, 416.
26 A. D. Irwin, J. S. Holmgren and J. Jonas, *J. Mater. Sci.*, 1988, **23**, 2098.

Paper 9/04109E